Enhanced substrate-induced coupling in two-dimensional gold nanoparticle arrays

N. Félidj,* J. Aubard, and G. Lévi
Interfaces, Traitements, Organisation et Dynamique des Systèmes – CNRS UMR 7086, 1, rue Guy de la Brosse, 75005 Paris, France

J. R. Krenn, G. Schider, A. Leitner, and F. R. Aussenegg
Institut für Experimentalphysik, Karl Franzens University, Universitätplatz 5, A–8010 Graz, Austria
(Received 14 May 2002; published 6 December 2002)

The influence of substrate induced coupling on plasmon excitations is probed by means of visible and near-infrared extinction microspectroscopy on various arrays of gold oblate spheroidal particles deposited onto a 20-nm-thick gold film. At zero incidence angle and for an interparticle spacing smaller than 250 nm, the spectra exhibit two bands instead of the single one observed for similar particles but deposited on indium tin oxide coated glass. We suggest that the short-wavelength band proceeds from two simultaneous mechanisms: (i) Excitation of a surface-plasmon resonance localized on the particles. (ii) Generation at the gold-glass interface of a propagating surface-plasmon wave due to the fact that the gold particles can act as a grating coupler. Surface-enhanced Raman-scattering experiments performed on oblate spheroid arrays give arguments in favor of the attribution of the long-wavelength band to surface-plasmon resonance of an ensemble of strongly coupled particles. When increasing the spacing between particles of the array beyond 250 nm, extinction spectra display the emergence of a new band. Calculations suggest that this new band proceeds from the excitation of a surface-plasmon standing wave on the film due to Bragg scattering. This assignment to Bragg scattering is supported by the investigation of the effect of varying the incidence angle under both transverse magnetic and transverse electric polarizations.

DOI: 10.1103/PhysRevB.66.245407 PACS number(s): 78.67.Bf, 78.66.Vs

I. INTRODUCTION

Noble-metal particles of sub-wavelength size (*nanoparticles*) can sustain resonances of collective electron oscillations known as *localized surface plasmons* (LSP's).[1] The excitation of LSP's leads to the emergence of strong extinction bands and to a giant amplification of the local electromagnetic field. These effects are of high general interest in the context of future optical device applications such as guiding light on the sub-micrometer scale,[2] optical spectroscopy such as second-harmonic generation,[3] and surface enhanced Raman scattering.[4]

For a *single isolated* particle, the individual plasmon resonance depends on the particle size and shape as well as on the dielectric functions of the particle and the surrounding medium.[1] For any assembly of particles that are commonly used for experiments, the properties of individual particles are considerably modified on account of the interaction with the substrate and with other particles.[5–12] Electromagnetic coupling between particles can arise both from very short-distance interaction and from long-range interaction. Near-field coupling occurs for close particles in the order of some tens of nanometers,[5,13] and can produce a strong confinement of the local electric field,[14] while far-field coupling is mediated via scattered light fields that are of dipolar character. Most of the previous investigations on the optical properties of gold nanoparticles arrays were performed on insulating or only weakly conducting substrates; generally a rather weak far-field dipolar coupling was found.[5,8,10–12] However, recently published results show that enhanced interaction between particles may occur, provided the structure of the underlying surface can mediate propagating waveguide modes.[5,11,15–18]

In this paper, we report on the strong coupling between nanoparticles mediated by surface-plasmon waves propagating on a gold film. In this purpose, the extinction spectra of gold nanoparticles regularly arranged as square arrays onto a flat gold film are investigated such that the effect of the substrate on the interaction between particles can be probed. Spectra of gold oblate spheroids on gold film display two or three bands instead of the single one observed for similar arrays but deposited on indium tin oxide coated glass. We suggest some explanations for the origin of these bands based on the comparison with spectra of elongated ellipsoid arrays, surface-enhanced Raman-scattering experiments, grating coupling, and Bragg scattering calculations.

II. EXPERIMENTAL TECHNIQUES

Our samples are constituted of square arrays of gold particles deposited on a smooth gold film whose thickness (20 nm) enables us to measure the optical spectra in transmission mode. The shape of the particles approaches oblate spheroids, the major axis of which lies along the gold film. These samples were fabricated by electronic beam lithography using a modified JEOL 6400 scanning electronic microscope equipped with a software driving the electron beam.[8,19] The whole array size is a square of 100 or 200 μm side. Absorption spectra were obtained from a LOT-ORIEL model MS260*i* spectrometer (260 mm focal length) with a 1024-diode array detector thermoelectrically cooled. This spectrometer is coupled by fiber optics to a LEITZ microscope equipped with a $50\times$ objective of 0.55 numerical aperture. The light source is a halogen lamp illuminating the sample with an almost collimated beam. The investigated array zone is limited by a small hole to a radius of approximately

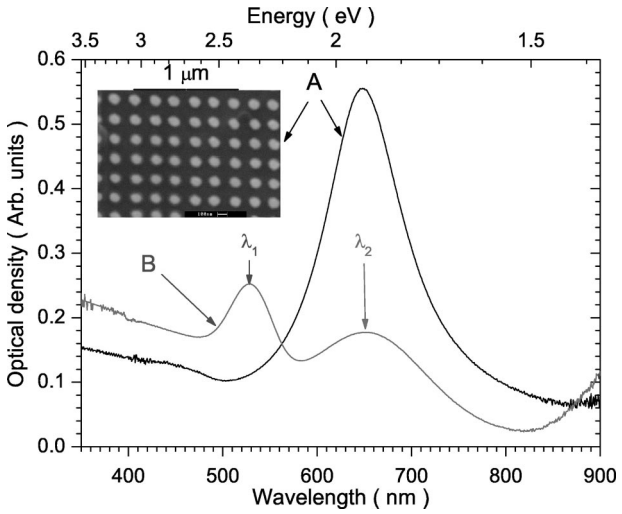

FIG. 1. Extinction spectrum of arrays of gold oblate spheroidal particles deposited on ITO (major axis 110 nm parallel to the ITO substrate, minor axis 60 nm perpendicular to the ITO, interparticle spacing $\Lambda = 200$ nm) (spectrum *A*), and a 20-nm gold film (major axis 120 nm parallel to the gold film, minor axis 44 nm perpendicular the gold film, interparticle spacing $\Lambda = 200$ nm) (spectrum *B*). The inset displays a scanning electronic microscopy image of the array of gold particles on ITO.

50 μm. Raman spectra are recorded in backscattering geometry on a DILOR *XY* microspectrometer constituted by a double monochromator used in subtractive mode to select a given spectral range and a third monochromator giving the dispersion. The detector is a thermoelectrically cooled charge coupled device (Jobin Yvon CCD, 1024×256 pixels). The excitation is obtained with either an Ar^+ model 165 or a He/Ne model 107/207 spectra physics lasers. In order to avoid any grating degradation, the laser power never exceeds 50 mW at the sample.

III. RESULTS AND DISCUSSION

A. Assignment of the extinction bands

In Fig. 1, we compare the extinction spectrum of two similar arrays of gold oblate spheroidal particles. In spectrum *A*, the spheroidal particles (110-nm major axis and 60-nm minor axis) are deposited as a square array onto indium tin oxide (ITO) with 200 nm interparticle spacing Λ. In spectrum *B*, the particles (120 nm and 44 nm major and minor axes, respectively) are deposited onto a gold film with the same interparticle spacing. The complete different aspect of these two spectra (Fig. 1) are unlikely to result from the slight differences in the size and shape of these two gratings. For spectrum *A*, a single plasmon band located at 650 nm is observed as expected from the circular symmetry of the spheroid.[12] Conversely, spectrum *B* exhibits two maxima separated by a wide dip: The short-wavelength maximum (λ_1) is located at 525 nm and the long-wavelength one (λ_2) at approximately 650 nm. The position of this second maximum at the same wavelength (650 nm) as that of arrays of similar particles on ITO is fortuitous. These two maxima that do not change with the incident light polarization look like those observed by Freeman and co-workers[20] for spherical gold particles immobilized on a silanized glass substrate. These authors attributed the first band at 525 nm to surface-plasmon localized on individual gold particles and the second one, shifted towards much longer wavelengths, to a plasmon resonance of a set of particles resulting in a strong dipole-dipole coupling due to the particle closeness. When inspecting our experimental spectra, the first arising question is: Are these two maxima due to extinction bands or to the occurrence of a dip originating in a destructive interference phenomenon? In such a process, the incident light can interfere destructively either with the image field,[21] or with a propagating wave guide mode resonant to the particle plasmon.[16] When increasing the inter particle distance, the energy of the dip should not change in the former case,[21] or decrease in the latter one.[16] Since this is not the case (see Fig. 4, we can conclude that the two maxima of spectrum *B* in Fig. 1 reflect two extinction bands.

We propose to assign the two bands observed in spectrum *B* in Fig. 1 according to the Holland and Hall interpretation of reflectivity spectra of silver and gold island films deposited on a continuous silver film via various thickness spacers of lithium fluoride (LiF).[22] The silver island absorption resonance (at 400 nm) was found to fall very close to the asymptotic surface-plasmon wavelength for silver at 350 nm. Replacing silver islands by gold ones, these authors observed two minima at 350 nm and 540 nm. They assign the 540-nm minimum to a gold particle resonance and the 350-nm minimum to the excitation of a propagating surface-plasmon mode. For a semi-infinite metal, the surface plasmon propagating wavelength arising from a grating coupling mechanism is given[23] by

$$k_{sp} = \frac{\omega}{c}\left(\frac{\varepsilon_1 \varepsilon_2}{\varepsilon_1 + \varepsilon_2}\right)^{1/2} = \frac{\omega}{c}\sin\theta_i \pm mG. \qquad (1)$$

In Eq. (1), k_{sp} is the amplitude of the surface-plasmon wave vector, ω the angular frequency of the incident light beam, c the speed of light in vacuo, θ_i the incidence angle, m an integer, $G = 2\pi/\Lambda$ the amplitude of the grating vector, ε_1 and ε_2 the dielectric functions of the metal and the surrounding medium, respectively. In the case of spectra of gold particles on a gold film (spectrum *B* in Fig. 1), the calculations were performed using the experimental gold dielectric function.[24] For the array considered here, the particle spacing is $\Lambda = 200$ nm and the predicted wavelength value is 513 nm for the first grating order, which is close to the 525 nm of the experimental band (see Table I).

Nevertheless, 525 nm is also the wavelength at which is usually observed the LSP resonance of individual gold particles.[1,21] In order to check whether the 525 nm band observed in spectrum *B* in Fig. 1 could arise from such a LSP, we recorded spectra of square arrays of elongated gold ellipsoidal particles deposited on ITO and gold films. On ITO, spectra display two bands polarized at 90 deg of each other along the two principal ellipsoid axes (Fig. 2). The band located at 580 nm and polarized along the ellipsoid medium axis (transverse polarization) is due to a localized surface-plasmon excitation corresponding to the particle medium

TABLE I. Calculated wavelengths [Eq. (1)], λ_{GC} in nanometers, at which a grating coupling occurs.

Interparticle spacing (nm)	λ_{GC} (nm) at air gold interface		λ_{GC} (nm) at gold glass interface	
	$m=1$	$m=2$	$m=1$	$m=2$
180	363		509	499
200	369		513	500
230	380		522	502
250	399		530	503
300	465	325	558	504
320	480	330	574	505

axis polarizability tensor component. In the same way, the long-wavelength band at 750 nm, polarized along the major axis (longitudinal polarization) is attributed to a particle surface plasmon along this axis. When elongated particles are deposited on a gold film, the extinction spectrum exhibits three bands at 540 nm, 650 nm, and 755 nm (Fig. 3). Two of them are polarized: that at 540 nm along the particle medium axis, and that at 650 nm along the major axis. The third band (755 nm) is unpolarized (Fig. 3). The bands polarized along the ellipsoid principal axes can be assigned to LSP.[1] Accordingly, this result suggests us that the band observed at 525 nm in spectrum *B* of Fig. 1 for oblate spheroids can also proceed from a LSP. The origin of the unpolarized band at 755 nm will be discussed below.

Under longitudinal polarization, the band at 540 nm is not completely quenched since a broad shoulder is still visible (Fig. 3, spectrum *C*), while under transverse polarization, no band can be longer observed at 650 nm (Fig. 3, spectrum *B*). We can then suppose that the broad shoulder remaining at approximately 540 nm under longitudinal polarization arises from the excitation of the surface-plasmon wave traveling at the gold-glass interface (Table I).

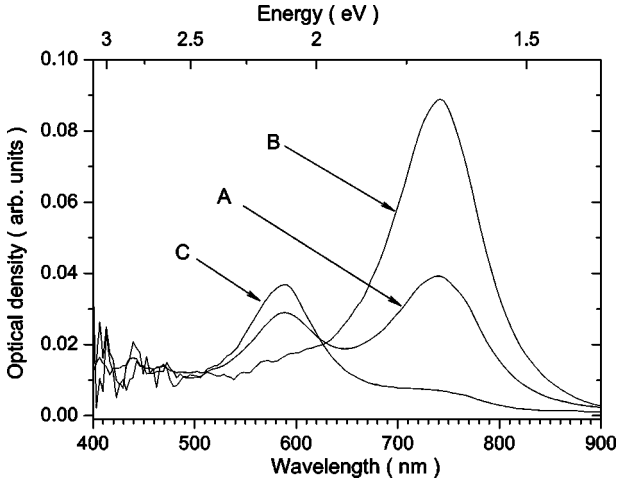

FIG. 2. Extinction spectrum of arrays of gold elongated ellipsoidal particles deposited on ITO (major axis 145 nm and medium axis 80 nm are both parallel to the ITO substrate, minor axis 30 nm is perpendicular to the ITO, interparticle spacing $\Lambda \simeq 490$ nm). Spectrum *A*: unpolarized incident light beam, spectrum *B*: polarization along the particle major axis, and spectrum *C*: polarization along the medium axis.

We thus suggest the occurrence of two simultaneous mechanisms for explaining the band displayed at 525 nm in Fig. 1, spectrum *B*: (i) the resonance of isolated surface-plasmon localized on the particles and (ii) the excitation of a propagating surface-plasmon wave at the gold-glass interface; this latter excitation can occur because the particles can act as surface roughness and couple the incident radiation to the surface plasmon.[22]

We wonder now about the assignment of the second extinction band appearing in spectra of gold oblate spheroid array on gold and located in spectrum *B* in Fig. 1 at 650 nm. A simple explanation is that this band comes from a plasmon

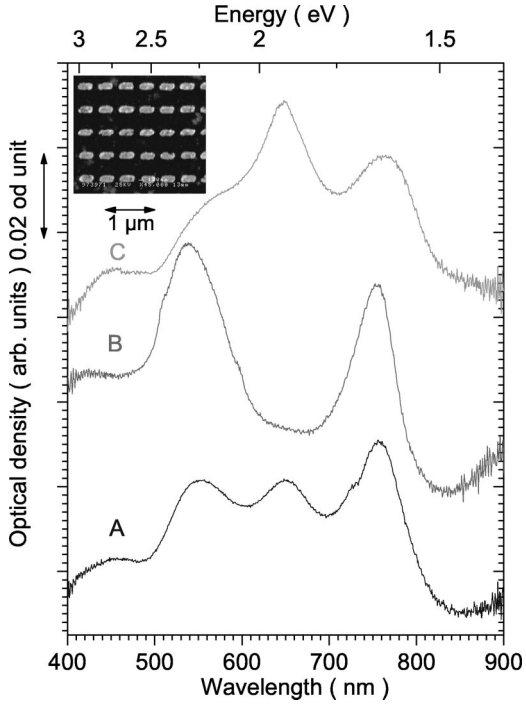

FIG. 3. Extinction spectra of gold elongated ellipsoidal particles deposited as a square array on a 20-nm-thick gold film. Particle major and medium axes parallel to the substrate are 400 nm and 100 nm, respectively, minor axis perpendicular to the substrate is about 30 nm. The spacing between particles is approximately $\Lambda \sim 300$ nm. Spectrum *A*: Unpolarized incident light beam, spectrum *B*: polarization along the medium axis (transverse polarization), spectrum *C*: polarization along the major axis (longitudinal polarization). Spectra have been vertically displaced for clarity. The inset displays a scanning electronic microscopy image of the array.

excitation of an ensemble of coupled particles. In a sense the assignment of this band would be similar to that given for silanized gold plates.[21] To support this assumption, we performed surface-enhanced Raman-scattering (SERS) experiments on the array of Fig. 1, spectrum *B*. It is generally admitted that the main mechanism leading to the SERS effect is a giant amplification of the electric field due to plasmon resonances of an ensemble of coupled particles.[4] Evidence of such a SERS effect on the studied arrays would be a strong argument in favor of the assignment of the 650-nm extinction band to surface-plasmon excitation of coupled particles. The investigated molecule was the *trans*-1,2−bi-(4−pyridyl) ethylene (BPE), which was already found to be very efficient molecular probe in SERS experiments.[12,21] These Raman spectra experiments were performed using the 632.8-nm excitation line of an He-Ne laser (3 mW power at the sample) that lies within the extinction band at 650 nm. A strong Raman signal is observed with a gain per molecule estimated in the order of 10^6. We may thus propose that the band at 650 nm arises from surface-plasmon excitation of an ensemble of coupled particles. Accordingly, the extinction band observed at 755 nm for elongated particles may be attributed to the resonance of an ensemble of coupled particles (Fig. 3).

Let us now consider what could be the mechanism at the origin of the very strong coupling between particles since the dipole-dipole coupling appears too weak to give rise to the band at 650 nm because of the rather large spacing between particles. The most likely hypothesis is the excitation of propagating surface-plasmon waves at either side of the gold film. We have already mentioned that the band at 525 nm might arise from the excitation of a surface-plasmon wave traveling at the gold-glass interface under a grating mechanism.[23] In the same way, gold particles may couple the incident radiation at the air-gold interface in the UV spectral region (Table I). No band corresponding to this process is observed, probably on account of a strong interband damping.

SERS experiments performed using the 514.5-nm excitation of an argon-ion laser show no signal of the BPE molecule, even under long integrating time (30 min) and rather large laser power at the sample (50 mW). The absence of any SERS spectrum under 514.5-nm excitation can be explained by the well-known observation of a very much weaker field enhancement on individual particles than on coupled ones,[4] and by the fact that a fraction of the band at 525 nm comes from a surface plasmon propagating at the gold-glass interface.

From the foregoing discussion, we thus suggest the following process to explain the occurrence of two extinction bands in spectrum *B*, Fig. 1.

(i) Incident light excites simultaneously a traveling surface plasmon by a grating coupling mechanism and a localized particle resonance. These simultaneous excitations are at the origin of the short-wavelength band observed at 525 nm.

(ii) The propagating mode couples energy back into distant nanoparticles.

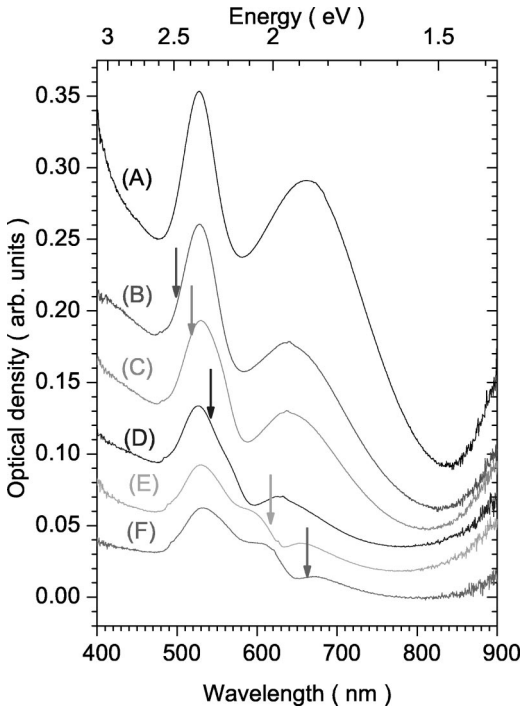

FIG. 4. Extinction spectra of arrays of gold oblate spheroidal particles identical to those of spectrum *B*, Fig. 1, deposited on a 20-nm gold film for different spacing between particles: spectrum *A*: $\Lambda = 180$ nm, spectrum *B*: 200 nm, spectrum *C*: 230 nm, spectrum *D*: 250 nm, spectrum *E*: 300 nm, spectrum *F*: 320 nm. Spectrum *F* is vertically lowered by 0.03 density unit for clarity. Arrays display the wavelengths at which the Bragg scattering condition [Eq. (2)] is fulfilled.

(iii) A fraction of this energy is absorbed and scattered by particles leading to the long-wavelength band at approximately 650 nm.

B. Study of the coupling strength

Whatever is the involved mechanism for particle interaction, increasing the distance between particles results in a decreasing of the coupling. In the mechanism we propose, this coupling is mediated by surface-plasmon traveling waves. The strength of such a coupling between particles depends on the propagation length of the surface mode, whose intensity decreases as $\exp(-\alpha r)/\sqrt{r}$,[15] where α describes the propagation length of the mode. Lamprecht and co-workers[2] have evaluated this propagation length to be in the order of 10 μm, therefore large enough to couple a great number of particles within the array. In order to probe the influence of the distance between particles, we study now various arrays constituted of identical gold particles deposited at increasing distances on a gold film. A decrease in the coupling between particles would manifest itself by a shift of the long-wavelength band (λ_2) towards smaller wavelengths, according to the general observation of the decrease of the eigenmodes splitting when coupling between modes is reduced. Figure 4 shows extinction spectra of identical gold oblate spheroidal particles (major axis: 120 nm, parallel to substrate plane, minor axis: 44 nm, perpendicular to sub-

strate plane) deposited onto a 20-nm-thick gold film at different interparticle spacings Λ. As expected, increasing the interparticle spacing from 180 nm to 250 nm brings about a shift towards shorter-wavelengths of the λ_2 band. On the other hand, the short-wavelength band λ_1 remains at the same wavelength. Besides, on increasing the interparticle spacing from 180 nm (spectrum *A*) to 320 nm (spectrum *E*), one notices the weakening of the overall extinction coefficient resulting from the decrease of the particle density. These features all together reflect the weakening of the coupling between particles according to the exponential decrease of the surface mode intensity with distance.

A new interesting feature is the emergence, in spectrum *D* ($\Lambda = 250$ nm), of a shoulder located approximately at 550 nm. In spectra *E* ($\Lambda = 300$ nm) and *F* ($\Lambda = 320$ nm), this new contribution develops clearly as a third band (λ_3) located at about 600 nm and 620 nm, respectively.

To interpret the physical origin of this new band, let us consider optical wave of incident light propagating normal to the gold film surface, which has been corrugated by depositing gold nanoparticles. If the surface-plasmon wave vector is equal to half the grating vector, Bragg scattering results in both forward and backward traveling waves that interfere to set up standing waves. Two configurations occur, one has field extrema on the film, the other has field extrema on the particles. The two branches of the dispersion relation have been calculated by Barnes and co-workers up to third order in Kd, where $K = G/2$ is the Bragg vector amplitude and d the corrugation amplitude:[25]

$$(k_{sp}^{\pm})^2 = \left(\frac{\omega}{c}\right)^2 \left(\frac{\varepsilon_1 \varepsilon_2}{\varepsilon_1 + \varepsilon_2}\right)[1 - (Kd)^2] \pm 2Kd \frac{K^2}{\sqrt{-\varepsilon_1 \varepsilon_2}}\left[1 - \frac{7}{2}(Kd)^2\right], \qquad (2)$$

where symbols have the same meaning as in Eq. (1). Using the relation [Eq. (2)], we determined the energy $\hbar\omega$ of the incident photon at which Bragg scattering should occur, that is, the energy at which $\overline{k_{sp}} = K = G/2$, where $\overline{k_{sp}} = 1/2\sqrt{(k_{sp}^{+})^2 + (k_{sp}^{-})^2}$ corresponds to the central position of the gap between the upper and the lower branches of the relation of dispersion. In this self-consistent calculation, we used the experimental gold dielectric function[24] and a corrugation amplitude equal to half the height (22 nm) of the particles. This position, expressed in wavelength units, is displayed in Fig. 4 as arrows. Since, in our experiments, the incident beam contains all the wavelengths within a given spectral range, those photons that match both the energy and momentum of the surface plasmons at the air-gold interface should be preferentially absorbed, giving rise to the third band. Probably on account of the approximations considered in the theory,[25] the agreement between experimental and calculated wavelengths is rather approximate. As increasing the interparticle spacing Λ, the calculated wavelengths move towards longer wavelengths faster than do the experimental ones. However, the experimental and calculated wavelengths vary in a similar way, supporting the assumption that the third band does arise from excitation of a surface-plasmon standing wave.[25] We can also remark that the emergence of the third band seems to reject the second one to longer wavelengths [spectra *E* and *F*], suggesting an increasing of the coupling between particles when Bragg scattering occurs. This is consistent with the fact that in one of the standing wave configuration, the electric field is maximum on the particles.[25] This enhanced field on the particles couples to the film, thus producing a stronger surface-plasmon wave according to the suggested mechanism given at the end of Sec. III A.

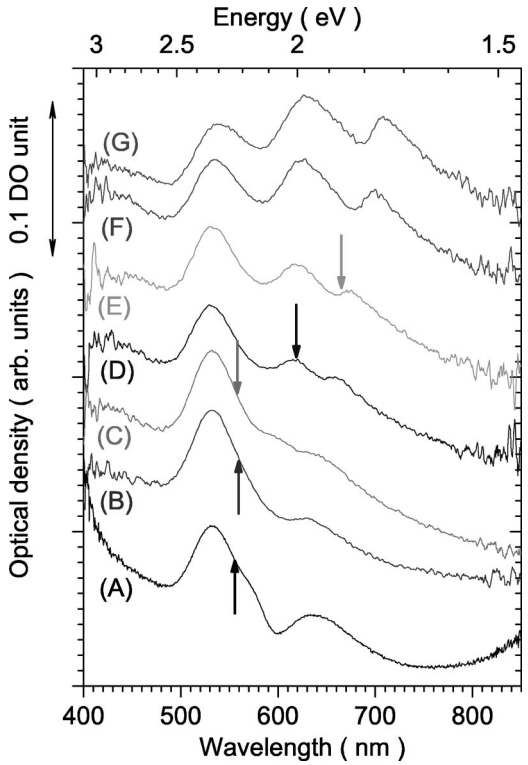

FIG. 5. Extinction spectra of grating *D* ($\Lambda = 250$ nm) as a function of the incidence angle under TM polarization. $\Lambda_{eff} = \Lambda/\cos\theta_i$: Spectrum *A*: $\theta_i = 0$ deg, *B*: 10 deg, $\Lambda_{eff} \simeq 254$ nm, *C*: 20 deg, $\Lambda_{eff} \simeq 266$ nm, *D*: 34 deg, $\Lambda_{eff} \simeq 301.5$ nm, *E*: 40 deg, $\Lambda_{eff} \simeq 326$ nm, *F*: 50 deg, $\Lambda_{eff} \simeq 389$ nm, *G*: 55 deg, $\Lambda_{eff} \simeq 436$ nm. Spectra have been vertically displaced for clarity. Arrows display the wavelength at which the Bragg scattering condition is fulfilled, calculated from [Eq. (2)].

C. Influence of changing incidence angle and polarization

In order to gain some supplementary information on the excitation of surface-plasmon waves on the gold film, we investigate the effect of polarizing the incoming electric field parallel [transverse magnetic (TM) polarization] or perpendicular [transverse electric (TE) polarization] to the incidence plane. Figure 5 displays the extinction spectra of the array *D* ($\Lambda = 250$ nm, Fig. 4) for various incidence angles under TM polarization. These spectra exhibit the emergence of a third band that shifts maximum towards longer wavelengths as increasing the incidence angle from $\theta_i = 0$ deg to $\theta_i = 55$ deg. Spectra of similar arrays on ITO (spectrum *A* in Fig. 1) do not change when increasing the incident angle of

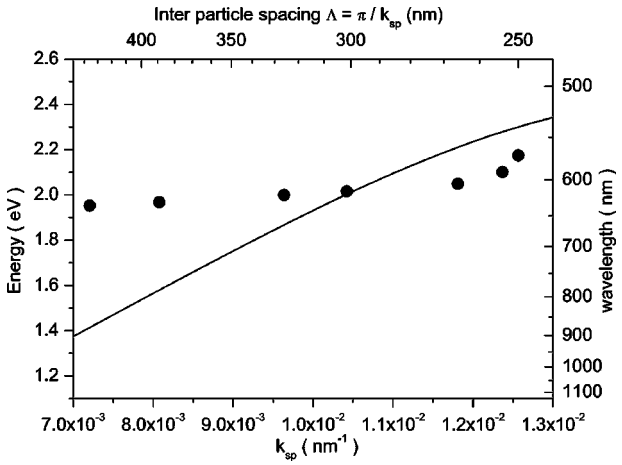

FIG. 6. ● ● Energy (eV) of the third band appearing in Fig. 5 as a function of the surface-plasmon wave vector amplitude $k_{sp}=G/2$, where $G=2\pi/\Lambda_{\text{eff}}$ is the effective lattice vector. Full line gives the position in energy (eV) at which Bragg scattering condition is fulfilled, calculated from Eq. (2) for grating *D* at various effective interparticle spacings Λ_{eff}.

the light impinging on the array, neither under TM nor under TE polarizations. This result rules out the possibility for the third band to arise from the fact that under nonzero incidence angle the intersection of the plane wave with the spheroidal particle is no longer a circle resulting in a degeneracy lift of the particle polarizability.

When comparing experiments performed on enlarging the interparticle spacing at 0 deg incident angle (Fig. 4) with those obtained when increasing the incident angle at constant particle spacing (Fig. 5), we notice that the spectra behave in a similar way showing the emergence of a third band that shifts towards longer wavelengths. We therefore suggest that increasing the incident angle can be thought of as introducing an *effective interparticle spacing* Λ_{eff}. If the incident light of k_0 wave vector ''experiences'' a grating wave vector *G* at zero incident angle, it can be assumed that it ''experiences'' a grating wave vector $G\cos\theta_i$ at incidence θ_i. The effective interparticle spacing Λ_{eff} can thus be considered as equal to $\Lambda_{\text{eff}}=\Lambda/\cos\theta_i$. Using this effective interparticle spacing Λ_{eff}, we calculated the wavelengths at which the Bragg scattering should occur,[25] which are shown as arrows on the Fig. 5. The calculated wavelengths vary in the same way when increasing the incidence angle, i.e., the effective interparticle spacing. Figure 6 displays a ''*dispersion curve*'' obtained by plotting the energy of the band attributed to Bragg scattering as a function of the amplitude of the surface-plasmon wave vector $\overline{k_{\text{sp}}}$ for which Bragg scattering occurs. For comparison, we also give in Fig. 6 the energy at which Bragg scattering condition is fulfilled, calculated from Eq. (2) when the interparticle spacing is varied: The calculated curve accounts for the energy increase of the third band with the surface-plasmon wave vector.

The various spectra recorded under TE polarization differ completely from those obtained under TM polarization. Except from a very slight shift towards short wavelength of the second band, increasing the incidence angle has no effect on

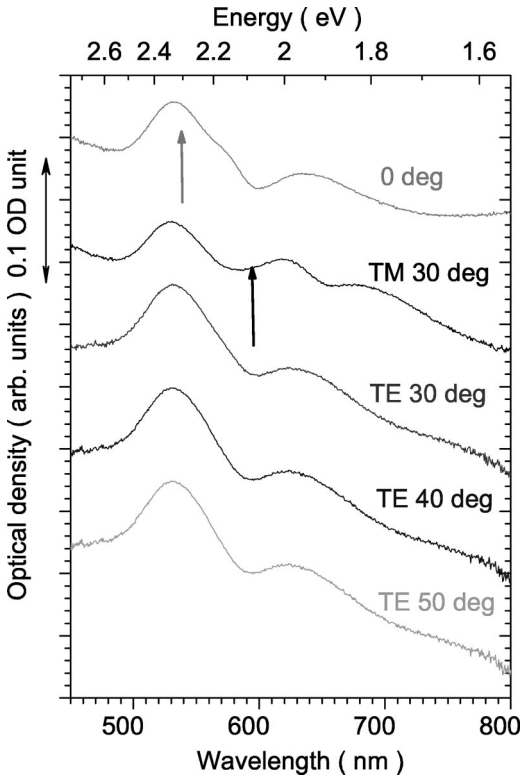

FIG. 7. Comparison between the extinction spectra of grating *D* ($\Lambda=250$ nm) for various incidence angles under TE and TM polarizations. Spectra were vertically displaced for clarity. Arrows display the wavelength at which the Bragg scattering condition is fulfilled, calculated from [Eq. (2)].

the extinction spectra under TE polarization: No third band appears whatever is the angle of the incident light (Fig. 7). Under the assumption that coupling proceeds from energy transfer of surface plasmons localized on the particles to the film, the propagating surface waves should be generated whatever is the polarization state of the incident light wave. Under TE polarization, the standing surface plasmons on the film, which are of TM nature, cannot be strongly coupled with incident light, thus leading to spectra that do not exhibit the third band (λ_3). Unlike this, under TM polarization, incident light can match energy and momentum of the surface standing waves, thus leading to the emergence of the third band in the extinction spectrum. These reasons allow us to conclude that the third band does arise from a surface-plasmon standing wave, which is generated by energy transfer from plasmons localized on the particles when the Bragg condition is fulfilled.

IV. CONCLUSION

In this paper we have reported on the extinction spectra of gold oblate spheroidal nanoparticle arrays regularly arranged onto a flat gold film. We showed that, unlike the same arrays deposited on ITO coated glass, the extinction spectra exhibit several extinction bands: the comparison of these spectra with previous results[22] leads us to attribute the short-wavelength band to ''*mixed mode*'' proceeding from the si-

multaneous excitation of localized and propagating surface-plasmon modes. This interpretation is supported by the comparison of the spectra of oblate spheroids with those of elongated particles, which display three bands, among which two are polarized along the particle principal axes parallel to the substrate. SERS experiments performed on these arrays using the BPE molecule as a probe speak in favor of the attribution of the second band, shifted towards longer wavelengths, to the excitation of an ensemble of particles, strongly coupled by a propagating surface-plasmon wave. Beyond an interparticle distance of 250 nm or when increasing the incidence angle, a third band emerges. Calculations using a dispersion relation established by Barnes and coworkers for dot arrays lead us to attribute this third band to the excitation of a plasmon standing wave on the gold film arising from Bragg scattering.[25]

ACKNOWLEDGMENTS

This work was possible due to the financial support from the French Foreign Office through a PAI Amadeus and the French Embassy in Vienna.

*Electronic address: Felidj@paris7.jussieu.fr

[1] U. Kreibig and M. Vollmer, *Optical Properties of Metal Clusters* (Springer, New York, 1995). C. F. Bohren D. R. Huffman, *Absorption and Scattering of Light by Small Particles* (Wiley, New York, 1983).

[2] B. Lamprecht, J. R. Krenn, G. Schider, H. Ditlbacher, M. Salerno, N. Félidj, A. Leitner, and F. R. Aussenegg, Appl. Phys. Lett. **79**, 51 (2001).

[3] B. Lamprecht, A. Leitner, and F. R. Aussenegg, Appl. Phys. B: Lasers Opt. **68**, 419 (1999).

[4] M. Moskovits, Rev. Mod. Phys. **57**, 783 (1985).

[5] M. Meier, A. Wokaun, and P. F. Liao, J. Opt. Soc. Am. B **2**, 931 (1985); E. T. Caron, W. Fluhr, M. Meier, A. Wokaun, and H. W. Lehmann, *ibid.* **3**, 430 (1986).

[6] P. A. Bobbert and J. Vlieger, Physica A **147**, 115 (1987).

[7] T. Yamaguchi, S. Yochida, and A. Kinbara, Thin Solid Films **21**, 173 (1974).

[8] W. Gotschy, K. Vonmetz, A. Leitner, and F. R. Aussenegg, Opt. Lett. **21**, 1099 (1996).

[9] M. S. Sander, R. Gronsky, Y. M. Lin, and M. S. Dresselhaus, J. Appl. Phys. **89**, 2733 (2001).

[10] G. Schider, J. R. Krenn, W. Gotschy, B. Lamprecht, H. Ditlbacher, A. Leitner, and F. R. Aussenegg, J. Appl. Phys. **90**, 3825 (2001).

[11] B. Lamprecht, G. Schider, R. T. Leichner, H. Ditlbacher, J. R. Krenn, A. Leitner, and F. R. Aussenegg, Phys. Rev. Lett. **84**, 4721 (2000).

[12] N. Félidj, J. Aubard, G. Livi, J. R. Krenn, M. Salerno, B. Lamprecht, G. Schider, A. Leitner, and F. R. Aussenegg, Phys. Rev. B **65**, 075419 (2002).

[13] J. C. Weeber, A. Dereux, C. Girard, J. R. Krenn, and J. P. Goudonnet, Phys. Rev. B **60**, 9061 (1999).

[14] J. R. Krenn, A. Dereux, J. C. Weeber, E. Bourillot, Y. Lacoute, and J. P. Goudonnet, Phys. Rev. Lett. **82**, 2590 (1999).

[15] H. W. Stuart and D. G. Hall, Phys. Rev. Lett. **80**, 5663 (1998).

[16] S. Linden, J. Kuhl, and H. Giessen, Phys. Rev. Lett. **86**, 4688 (2001).

[17] U. Schröter and D. Heitmann, Phys. Rev. B **60**, 4992 (1999).

[18] T. Kume, S. Hayashi, and K. Yamamoto, Phys. Rev. B **55**, 4774 (1997).

[19] M. Salerno, N. Felidj, J. R. Krenn, A. Leitner, and F. R. Aussenegg, Phys. Rev. B **63**, 165422 (2001).

[20] R. G. Freeman, K. C. Garbar, K. J. Allison, R. M. Bright, J. A. Davis, A. P. Guthrie, M. B. Hommer, M. A. Jackson, P. C. Smith, D. G. Walker, and M. J. Natan, Science **267**, 1629 (1995).

[21] A. Leitner, Z. Zhao, H. Bruner, F. R. Aussenegg, and A. Wokaun, Appl. Opt. **32**, 102 (1993).

[22] W. R. Holland and D. G. Hall, Phys. Rev. Lett. **52**, 1041 (1984); Phys. Rev. B **27**, 7765 (1983).

[23] H. Raether, *Surface Plasmons on Smooth and Rough Surfaces and on Gratings*, edited by G. Huhler, Springer Tracts in Modern Physics Vol. 111 (Springer, Berlin, 1988).

[24] B. Johnson and R. W. Christy, Phys. Rev. B **6**, 4370 (1972).

[25] W. L. Barnes, S. C. Kitson, T. W. Priest, and J. R. Sambles, J. Opt. Soc. Am. A **14**, 1654 (1997); S. C. Kitson, W. L. Barnes, and J. R. Sambles, Phys. Rev. Lett. **77**, 2670 (1996); W. L. Barnes, S. C. Kitson, T. W. Priest, and J. R. Sambles, Phys. Rev. B **54**, 6227 (1996); W. L. Barnes, T. W. Priest, S. C. Kitson, J. R. Sambles, N. P. K. Cotter, and D. J. Nash, *ibid.* **51**, 11 164 (1995).